Published in final edited form as:
Vib Spectrosc. 2011 November 1; 57(2): 338–341. doi:10.1016/j.vibspec.2011.08.005.

Depth-dependent Anisotropy of Proteoglycan in Articular Cartilage by Fourier Transform Infrared Imaging

Jian-Hua Yin, **Yang Xia***, and **Nagarajan Ramakrishnan**[1]
Department of Physics and Center for Biomedical Research, Oakland University, Rochester, MI 48309, USA

Abstract

Fourier transform infrared microscopic imaging (FTIRI) was used to quantitatively examine the anisotropies of proteoglycan (PG) and collagen in articular cartilage. Dried 6 μm thick sections of canine humeral cartilage were imaged at 6.25 μm pixel-size in FTIRI with an infrared analyzer set at 26 different angles between 0° and 180° polarization. Like the amide II and amide III peaks, the 1338 cm^{-1} band confirms the anisotropy of collagen fibrils in cartilage. The absorption profile of the sugar band shows an anisotropic flipping at the deeper part in the radial zone, just above the tidemark. Together with the reduction in the PG concentration and subsequent increase in tissue calcification in this region, this anisotropy flipping of sugar might be caused by the orientational change in the collagen-attaching PG from orthogonal to parallel when the fibrils are entering the calcified zone.

Keywords

sugar; proteoglycan; FTIRI; PCR; cartilage; imaging

1. Introduction

Proteoglycan (PG) is a principal macromolecular component in articular cartilage and embedded in the network of collagen fibrils in the tissue [1, 2]. Since the collagen network has a depth-dependent structure, which is commonly used to subdivide non-calcified cartilage into three histological zones from the articular surface to subchondral bone (superficial zone (SZ), transitional zone (TZ), and radial zone (RZ)), the PG concentration in cartilage is also depth-dependent [3]. Due to the strong water-binding ability of its sulfates, proteoglycan is responsible for the unique depth-dependent stiffness of cartilage as a soft load-bearing tissue in synovial joints [1, 4–6]. Either the disruption of the collagen network or a loss of any principal component would lead to the functional degeneration of cartilage, eventually shown as degenerative joint diseases such as osteoarthritis. Accurate determinations of the concentration and structure of the principal components in cartilage, therefore, are critically important.

*Corresponding Author and Address: Yang Xia, PhD, Department of Physics, Oakland University, Rochester, Michigan 48309, USA, Phone: (248) 370-3420, Fax: (248) 370-3408, xia@oakland.edu.
[1]Current Address: Defence Laboratory, Ratanada Palace, Jodhpur-342 011, Rajasthan, India

Fourier transform infrared imaging (FTIRI) is a new analytical imaging tool in biomedical research because of its fine resolutions in both spatial and spectral dimensions [7–15]. In the special dimension, the pixel resolution in FTIRI can be as fine as 5–10 μm in the standard configuration [12] and 1–2 μm when an attenuated-total-reflection device is used [16]. In the spectral dimension, FTIRI can distinguish many chemical groups that have different vibrational frequencies, such as amide I (centered around 1650 cm^{-1}), amide II (centered around 1550 cm^{-1}), amide III (centered around 1250 cm^{-1}) and sugar (centered around 1050 cm^{-1}) [7, 8, 12]. In most FTIRI studies in literature, the sugar component, which can be interpreted to represent proteoglycan, received little attentions since it had the weakest absorption and anisotropy in the middle infrared region [12, 14].

Based on our recent work that successfully quantified the percentage concentrations of both PG and collagen in cartilage by the combined FTIRI and the principal component regression (PCR) methods [17], this project re-analyzes the anisotropy characteristics of the sugar bands of the exiting FTIRI data where the sugar region had received little attention. In addition to the PCR-determined PG concentration profiles in cartilage, the 1338 cm^{-1} band of collagen II (the CH2 wagging vibration of proline side chains [8, 10, 11]) and the 1072 cm^{-1} band of PG (the sugar groups [7, 8]) were also included to examine the depth-dependent profiles of infrared absorbance.

2. Materials and methods

2.1 Specimen preparation and FTIRI Experiments

The detailed descriptions of the specimen preparation and FTIRI experiments were documented in a previous work [12]. Briefly, the rectangular blocks from 6 different canine humeral tissue included the whole thickness of articular cartilage that was still attached to the bone. The tissue blocks were embedded in paraffin and microtomed into 6 μm sections, which were mounted onto MirrIR slides (Kevley technologies, Chesterland, OH). These sections were de-waxed in three changes of xylene for 5 min each followed by re-hydration with de-ionized water. The sections were left to air dry at room temperature. The final 6 sections from 6 canines were not embedded with mounting media or cover glass when being imaged.

A PerkinElmer Spotlight 300 imaging system (Wellesley, MA) was used to image the specimen slides, which were mounted on a mechanical scanning stage in the reflectance mode. Rectangular regions of interest (ROI) in the tissue sections were selected for imaging, at 6.25 μm pixel resolution and 8cm^{-1} spectral step over a range of 4000-744 cm^{-1}. One IR wire-grid polarizer was inserted as the analyzer between the sample and the detector. The analyzer was rotated with a 5–10° increment over a range of 0–180° to obtain the anisotropic information of the specimen. Background absorbance was subtracted for each FTIRI measurement.

2.2 Data Analysis

The raw 3D data sets were re-analyzed by extracting the IR spectra in the spectra ranging of 4000-1000 cm^{-1} that were subsequently fed into a chemometrics software (Spectrum Quant + by PerkinElmer) which had a built-in PCR function [17]. Therefore, these extracted IR spectra from the FTIR image can be calculated to obtain their corresponding PG and collagen concentrations at any pixel location. All calculated PG concentrations in the specimen were converted in to the 2D PG concentration image. To improve the signal-to-noise ratio, 42 neighboring data points at the same depth location (column) were averaged as the PG concentration of this depth. Repeating this averaging at all tissue depths results in a depth-dependent profile of the PG concentration. In addition to the PCR-calculated PG

images and profiles, the 2D peak-area maps of collagen and PG were also obtained from the commercial software over a number of characteristic bands (1338 cm^{-1} band: 1355~1315 cm^{-1}, 1072 cm^{-1} band: 1125~1000 cm^{-1}) [7, 8, 10, 11].

3. Results

Fig 1 shows the visible image (a) and the corresponding chemi-maps of the 1338 cm^{-1} (b) and 1072 cm^{-1} (c) bands of one ROI in a tissue section, respectively. The PCR-calculated PG map is shown in Fig 1d, as well an IR spectrum from articular cartilage was drawn in Fig 1e. Although both chemi-maps visually assembled the distributions of collagen (by 1338 cm^{-1}) and PG (by 1072 cm^{-1}) in articular cartilage, their values (infrared absorptions) are qualitative and cannot be calibrated to the molecular concentrations quantitatively.

Fig 2 shows the depth-dependent profiles of the 1338 cm^{-1} and sugar (1072 cm^{-1}) absorption bands through the cartilage depth from the corresponding chemi-maps with the analyzer at 0° and 90°. The profiles of the un-polarized absorption across the same cartilage location are also included for comparison. In both 1338 cm^{-1} and 1072 cm^{-1} bands, the un-polarized profiles were always between the 0° and 90k profiles. In addition, the 1338 cm^{-1} profile is very similar to the profiles of amide II and amide III [13], which shows clearly an anisotropic flipping around the 70 μm depth (near the transitional zone). The PG (1072 cm^{-1}) profile does not exhibit any anisotropic flipping in the surface part of the AC tissue; however, it clearly shows an anisotropy flipping at about 580 μm depth, which is just above the tidemark in the tissue (Fig 2b). The similar result has been obtained for all tissue sections.

A particularly unique way of identifying the depth-dependent anisotropy is to use the anisotropy profiles [12, 13] from the imaging data, by plotting the average absorbance at the same tissue depth for all 26 analyzer angles and by fitting the absorption values to the following equation [12]: $A(r, \theta) = \pm A(r)\cos^2(\theta-\theta_0(r))+A_0(r)$, where r is the tissue depth (0 = articular surface), θ is the angle between the electric vectors of linear polarized light and transition moment vector, $A(r)$ and $A_0(r)$ are two depth-dependent scaling parameters. Fig 3 shows the anisotropy profiles of collagen (1338 cm^{-1} band) in both SZ (31.25 μm) and RZ (300 μm) tissue. The inversed sinusoidal feature between SZ and RZ clearly represents the perpendicular orientation of the collagen fibrils between SZ and RZ. As a comparison, the anisotropy of the sugar absorption (Fig 3b) also exhibits this inverted sinusoidal feature, not between SZ and RZ, but below and above the 580 μm tissue depth, which is just above the tidemark of the tissue. The anisotropic amplitude $A(r)$ were − 0.0082, 0.0020, 0.0027 and 0.0040 at 300, 606.25, 637.5 and 725 μm depths respectively, becoming bigger with the increase of tissue depth. $\theta_0(r)$ kept constant at ca. −19° at these depths.

4. Discussions

This is the first report that observes the anisotropy flipping of the sugar band just above the tidemark, which is near the interface between the uncalcified and calcified matrix. This phenomenon might be partly due to the reasons as the following. Based on the results of the electron microscopy, the PG show regular arrays orthogonal to the collagen fibrils in soft tissues [18, 19] and appear as complete hoops about the collagen fibril in the uncalcified tissue [19, 20]. In an electron microscopy study of the organization of proteoglycans and collagen fibrils in the human corneal stroma [23], PG was found to possibly form a repeating network of ring-like structures (~45 nm) around the collagen fibrils in the cross-sections, that is, a groups of six PG attached orthogonal to the circumference of the fibrils. In function, the chondroitin sulfate in PG has been considered to inhibit the calcification of soft connective tissues [18, 20, 21]. Based on the depth-dependent PCR-calculated PG

concentration profile shown in Fig 2b, the PG concentration in articular cartilage increases with the depth for most of the non-calcified cartilage. In the deep RZ below the 500 μm depth, the PG concentration began to reduce, which might weaken the inhibitory role of PG in the calcification process.

Thereby, the calcification process would enhance below the 500 μm depth when the collagen fibrils perpendicularly pass through the tidemark and approach the bone [22]. Around this deep tissue region, the orientation of the PG can change from orthogonally to axially parallel the collagen fibrils [18, 19]. The tightening of the PG binding to the collagen fibrils with an axially parallel orientation could increase the orientational order of the PG, which is being measured by the anisotropy parameter *A(r)* in this project.

In conclusion, FTIRI combining with the quantitative PCR calculation can analyze the structure and concentrations of the principal components in articular cartilage. The anisotropy of the collagen 1338 cm^{-1} band is consistent with those of amide II and amide III, showing an anisotropic flipping around the critical location near the tissue surface. The sugar band is seen to have an anisotropic flipping not near the surface but at the deepest part of RZ approaching the tidemark. Since the reduction of the chondroitin sulfate PG concentration and the increased amount of calcified material with the fibrils entering the calcified zone, this infrared anisotropy of sugar was attributed to the orientational changes in PG. This observation will be helpful to further understand the related structural and functional properties of connective tissues by the quantitative concentration calculation and anisotropies of principal components [17].

Acknowledgments

Grant Support: NIH R01 grants (AR 45172, AR 52353)

Yang Xia is grateful to the National Institutes of Health for the R01 grants (AR 045172, AR 052353).

References

1. Maroudas A. Nature. 1976; 260:808. [PubMed: 1264261]
2. Buckwalter JA, Mankin HJ. J Bone Joint Surg Am. 1997; 79:600.
3. Xia Y, Zheng SK, Bidthanapally A. J Magn Reson Imaging. 2008; 28:151. [PubMed: 18581328]
4. Chen SS, Falcovitz YH, Schneiderman R, Maroudas A, Sah RL. Osteoarthritis Cartilage. 2001; 9:561. [PubMed: 11520170]
5. Mow VC, Guo XE. Annu Rev Biomed Eng. 2002; 4:175. [PubMed: 12117756]
6. Wilson W, Huyghe JM, Donkelaar CCV. Biomechan Model Mechanobiol. 2007; 6:43.
7. Potter K, Kidder LH, Levin IW, Lewis EN, Spencer RG. Arthritis Rheum. 2001; 44:846. [PubMed: 11315924]
8. Camacho NP, West P, Torzilli PA, Mendelsohn R. Biopolymers. 2001; 62:1. [PubMed: 11135186]
9. David-Vaudey E, Burghardt A, Keshari K, Brouchet A, Ries M, Majumdar S. Eur Cell Mater. 2005; 22:51. [PubMed: 16307426]
10. Bi X, Yang X, Bostrom MP, Camacho NP. Biochim Biophys Acta. 2006; 1758:934. [PubMed: 16815242]
11. Bi X, Yang X, Bostrom MPG, Bartusik D, Ramaswamy S, Fishbein KW, Spencer RG, Camacho NP. Anal Bioanal Chem. 2007; 387:1601. [PubMed: 17143596]
12. Xia Y, Ramakrishnan N, Bidthanapally A. Osteoarthritis Cartilage. 2007; 15:780. [PubMed: 17317225]
13. Ramakrishnan N, Xia Y, Bidthanapally A. Phys Med Biol. 2007; 52:4601. [PubMed: 17634653]
14. Ramakrishnan N, Xia Y, Bidthanapally A, Lu M. Appl Spectrosc. 2007; 61:1404. [PubMed: 18198035]

15. Xia Y, Alhadlaq H, Ramakrishnan N, Bidthanapally A, Badar F, Lu M. J Struct Biol. 2008; 164:88. [PubMed: 18634884]
16. Yin JH, Xia Y. Biomed Opt Express. 2011; 2:937. [PubMed: 21483615]
17. Yin JH, Xia Y. Appl Spectrosc. 2010; 64:1199. [PubMed: 21073787]
18. Scott JE. Biochem J. 1988; 252:313. [PubMed: 3046606]
19. Scott JE, Haigh M. Biosci Rep. 1986; 6:879. [PubMed: 3103706]
20. Scott JE, Haigh M. Biosci Rep. 1985; 5:71. [PubMed: 3986311]
21. Scott JE, Orford CR. Biochem J. 1981; 197:213. [PubMed: 7317031]
22. Redler I, Mow VC, Zimny ML, Mansell J. Clin Orthop Related Topics. 1975; 112:357.
23. Muller LJ, Pels E, Schurmans LR, Vrensen GF. Exp Eye Res. 2004; 78:493–501. [PubMed: 15106928]

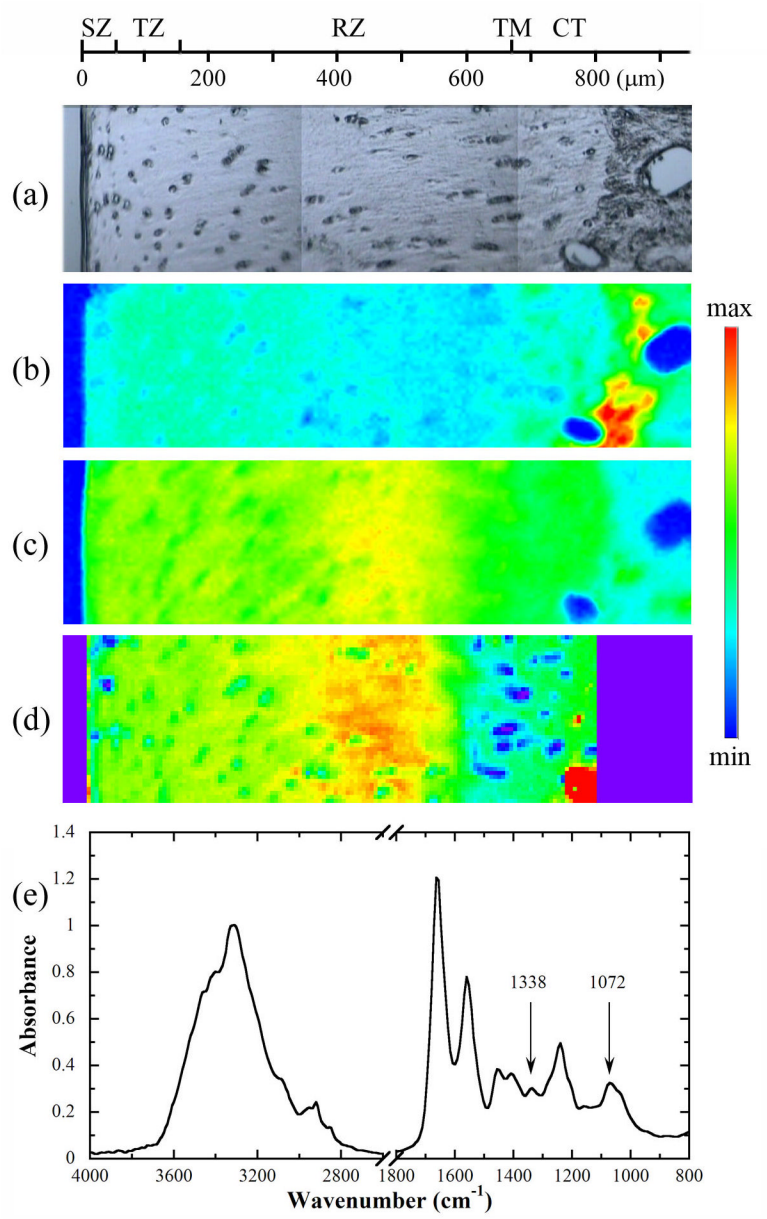

Fig 1.

(a) A visible image of a cartilage section, and the corresponding chemi-maps of (b) 1338 cm^{-1} and (c) sugar bands, both obtained without an analyzer. (d) The PCR-calculated PG concentration map with the min and max of 10 and 32%. (e) A FTIR spectrum extracted from the cartilage section. The scale maxima for the 1338 cm^{-1} and sugar chemi-maps are 0.045 and 0.1, respectively; the scale minimum is 0 in both chemi-maps. SZ: superficial zone, TZ: transitional zone, RZ: radial zone, CT: calcified tissue, TM: tidemark.

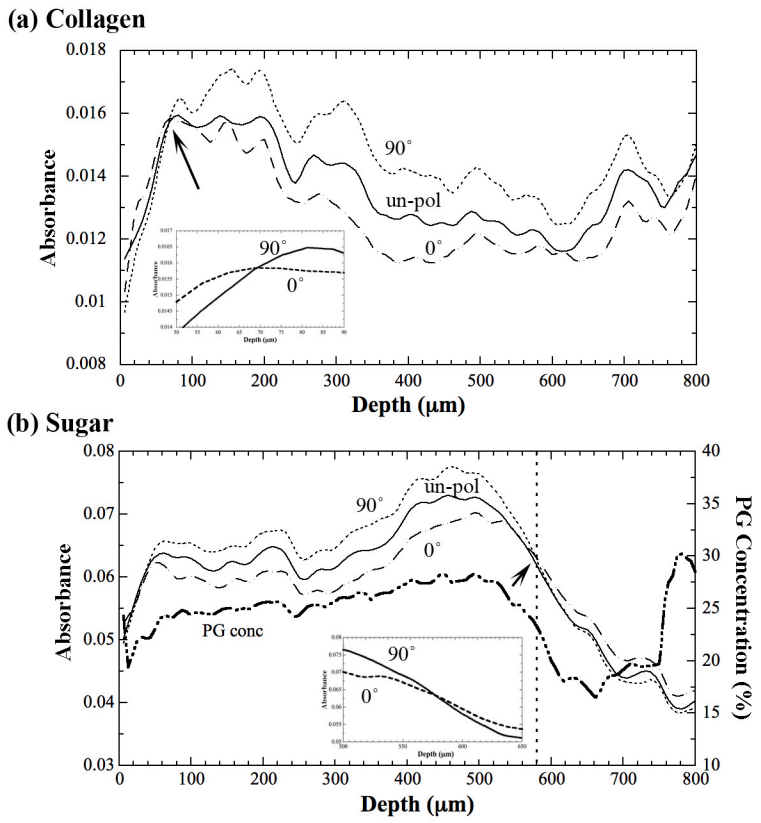

Fig 2.

The depth-dependent profiles of the infrared absorption intensities of (a) 1338 cm^{-1} and (b) sugar bands at 0° and 90° analyzer angles, and their comparison with the profiles without an analyzer, respectively. The concentration profile of PG by PCR algorithm is also shown in Fig 2b. The dotted line denotes the position of the anisotropic flipping of the sugar band. Two insets indicate the enlargements of the flipping regions.

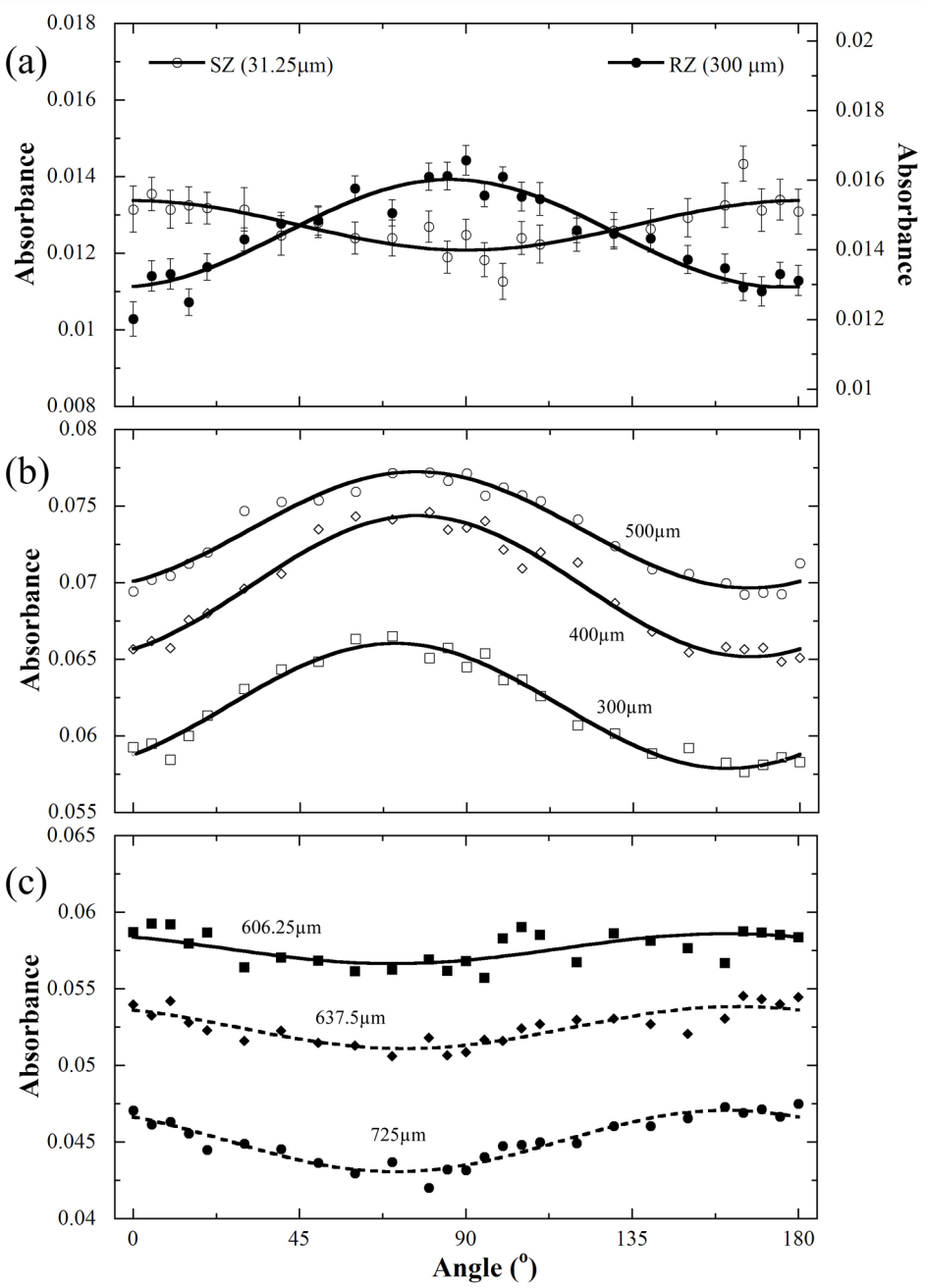

Fig 3.

The infrared absorbance anisotropies of (a) 1338 cm^{-1} at both 31.25 μm (SZ) and 300 μm (upper RZ) and (b) sugar bands at 300, 400 and 500 μm. (c) The infrared absorbance anisotropies of sugar band in the deeper RZ and calcified tissue (606.25, 637.5 and 725 μm). The mean errors of the sugar absorbance at the six depth locations from 300 to 725 μm are 9.7%, 8.4%, 6.0%, 7.5%, 9.9% and 8%, respectively.